

# Stabilization of an $\alpha$ Helix by $\beta$ -Sheet-Mediated Self-Assembly of a Macrocyclic Peptide\*\*

Yong-beom Lim, Kyung-Soo Moon, and Myongsoo Lee\*

The  $\alpha$  helix is an essential secondary structural motif in proteins. In particular,  $\alpha$  helices at the outer surface of proteins play an important role in specific biomolecular recognition events, such as in protein–DNA, protein–RNA, and protein–protein interactions.<sup>[1]</sup> The  $\alpha$ -helical structures are well stabilized in the context of intact proteins. However, an  $\alpha$ -helix-forming segment, when isolated from the protein as a short peptide, is rarely helical in solution owing to its inherent thermodynamic instability.<sup>[2]</sup> Because the stabilization of active folded forms of peptide is important for maintaining the unique functions of protein, extensive research into stabilized  $\alpha$ -helical peptides has been carried out.<sup>[3]</sup> Peptide helix stabilization approaches include the covalent cross-linking of amino acids located at the same face of an  $\alpha$  helix,<sup>[3a,b]</sup> hydrogen-bond surrogates,<sup>[2a]</sup> metal coordination,<sup>[3c]</sup> salt bridge formation,<sup>[3d]</sup> helix nucleation,<sup>[3e]</sup> helix capping,<sup>[3f]</sup> and synthetic  $\alpha$ -helix receptors.<sup>[3g]</sup>

These minimalist approaches have advantages with regard to simplicity and cost efficiency. However, when considering many  $\alpha$ -helix-mediated interactions occurring in a multivalent fashion,<sup>[4]</sup> the inherent limitation of such monomeric  $\alpha$ -helix approaches is that the complex and multivalent biological interactions cannot be effectively targeted.

Herein, we describe a simple but effective supramolecular approach in which multiple  $\alpha$ -helix-coated artificial proteins can be constructed by the self-assembly of simple peptides. Bottom-up self-assembly of functional supramolecular building blocks is a cost-efficient way of constructing bioactive multivalent structures.<sup>[5]</sup> To substantiate this goal, a building block was designed in such a way that both an  $\alpha$ -helical peptide segment and a self-assembling segment are located within a single macrocyclic structure (peptide 4, Figure 1a). As the self-assembling segment, a  $\beta$ -sheet peptide with predictable and well-known self-assembly behavior was selected. The  $\alpha$ -helix-forming segment is an alanine-based peptide. Lysines are located within the stretch of alanines to increase water solubility and to prevent aggregation.<sup>[6]</sup> The  $\beta$ -sheet peptide segment is a repeat of hydrophobic and of

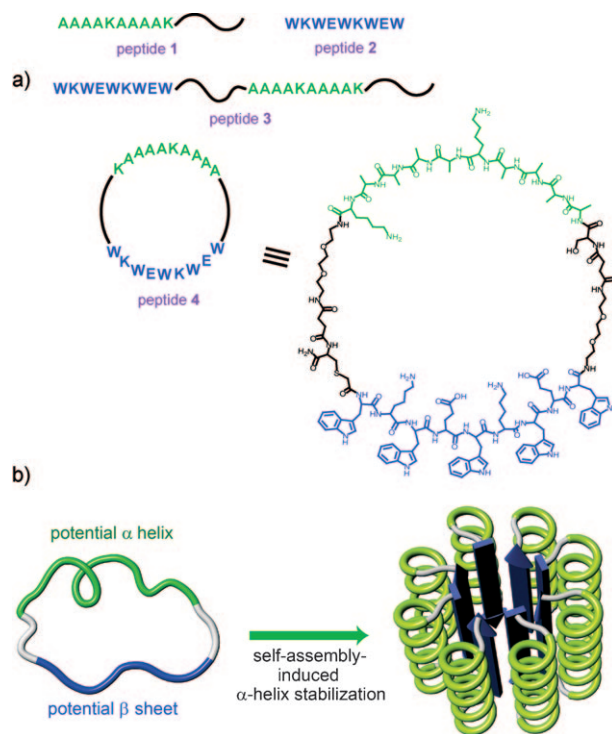


**Figure 1.** Self-assembly of macrocyclic peptides into an  $\alpha$ -helix-decorated artificial protein. a) Chemical structures. For detailed structures of all peptides, see the Supporting Information. Segments:  $\alpha$  helix, green;  $\beta$  sheet, blue; linker, black. b) The partially stabilized helical structure, which is further stabilized and multivalently presented on the surface of a nanostructure upon self-assembly of the  $\beta$ -sheet segment. Segments:  $\alpha$  helix, green;  $\beta$  sheet, blue; linker, gray.

positively or negatively charged amino acids. Such combination of amino acids promotes  $\beta$ -sheet hydrogen bonding and subsequent self-assembly into bilayered ribbon-like fibrous nanostructures.<sup>[7]</sup> Oligoethylene glycol-based linker segments are placed between the  $\alpha$ -helical- and  $\beta$ -sheet-forming sequences to decouple both segments. The peptide macrocycle was designed based on the hypotheses that 1) a cyclic structure will partially stabilize the helical structure by decreasing conformational entropy of the unfolded state,<sup>[8]</sup> and 2) a self-assembly-induced coil-to-rod transition in the  $\beta$ -sheet segment will further constrain and stabilize the helical structure (Figure 1b). The cyclization reaction was performed while protected peptide was still bound to the resin to achieve a pseudo-dilution effect and to reduce the entropic penalty associated with intramolecular cyclization<sup>[9]</sup> (Supporting Information, Figure S1).

We investigated the secondary structure of an only-helix-forming alanine-based segment, peptide 1, by circular dichro-

[\*] Dr. Y.-b. Lim, K.-S. Moon, Prof. M. Lee  
Center for Supramolecular Nano-Assembly and Department of Chemistry  
Yonsei University, Seoul 120-749 (Korea)  
Fax: (+82) 2-393-6096  
E-mail: mslee@yonsei.ac.kr  
Homepage: <http://csna.yonsei.ac.kr>

[\*\*] This work was supported by the National Creative Research Initiative Program of the Ministry of Education, Science and Technology.

Supporting information for this article is available on the WWW under <http://dx.doi.org/10.1002/anie.200804665>.

ism (CD) spectroscopy (see Supporting Information, Figure S2, for the full structure).  $\alpha$ -Helix formation is strongly dependent on temperature, with maximal helicity at low temperature, and unfolding occurs with increasing temperature. Even at low temperatures (1 °C), peptide **1** exhibited a strong negative band at 196 nm, indicating that the peptide is mostly in a random-coil conformation (Figure 2a). The  $\alpha$ -helical conformation of peptide **1** could only be stabilized when a helix-stabilizing agent, 2,2,2-trifluoroethanol (TFE), was used as a cosolvent and at low temperature (1 °C). Two negative bands at 204 nm and 220 nm and a strong positive band at about 190 nm were observed (Figure 2b). The small deviation from the characteristics of perfect  $\alpha$ -helical conformation (two negative minima at 208 nm and 222 nm) suggests that the helix is still only partially stabilized. As shown in Figure 2b, the temperature-induced helix-coil transition has a clear isodichroic point at 201 nm, which provides evidence for a simple two-state  $\alpha$ -helix and random-coil equilibrium.<sup>[3d]</sup> Taken together, the results indicate that peptide **1** is a poor helix former. Therefore, certain changes in molecular structure are necessary to stabilize the helical structure of peptide **1**.

Next, we examined the secondary structure of an only- $\beta$ -sheet-forming segment (peptide **2**). The CD spectrum (Figure 2a) shows a strong negative band at 212 nm, a strong

positive band at 197 nm, and a crossover point at 203 nm, indicating that the peptide is predominantly in a  $\beta$ -sheet conformation.<sup>[10]</sup> The  $\beta$ -sheet conformation of peptide **2** was found to be stable even at high temperatures (up to 81 °C; Supporting Information, Figure S4).

We then investigated the secondary structures in peptide **3**, a peptide that contains both of the  $\alpha$ -helical and  $\beta$ -sheet segments in a linear (acyclic) structure. Peptide **3** exists predominantly in a  $\beta$ -sheet conformation (Figure 2c). Peptide **4** is a cyclic peptide that is cyclized from the acyclic precursor peptide **3**. In clear contrast to the acyclic peptide **3**, the CD spectrum of the cyclic peptide **4** (Figure 2c) consists of a strong positive band around 190 nm ( $\alpha$  helix), strong negative bands at 204 nm and 207 nm ( $\alpha$  helix), a strong negative band at 214 nm ( $\beta$  sheet), and a weak shoulder at 223 nm ( $\alpha$  helix), indicating that both  $\alpha$ -helical and  $\beta$ -sheet conformations coexist. Considering the fact that the partially helical peptide **1** in the presence of TFE showed a negative band at 204 nm (see Figure 2b), the band of peptide **4** at 204 nm is likely come from the partially stabilized  $\alpha$ -helical conformation, or possibly from other types of intermediate helical structures (e.g. a polyproline type II helix or  $3_{10}$  helix). Taken together, these results clearly demonstrate that  $\beta$ -sheet formation between the macrocycles can stabilize an otherwise disordered  $\alpha$ -helical structure. It has been shown that  $\alpha$ -helical

segment of this type does not aggregate.<sup>[6]</sup> Thus, the formation of coiled-coil helix bundle structures should not be responsible for the stabilization of the  $\alpha$ -helix segment. Considering the fact that the acyclic peptide **3** is predominantly in  $\beta$ -sheet conformation, it is crucial that both segments are contained within the context of cyclic structure for the  $\alpha$ -helices to be efficiently stabilized by the  $\beta$ -sheet-mediated self-assembly process. It should be noted that peptide **4** showed essentially the same CD profile even after several months of incubation, indicating that it is a thermodynamically stable structure. The thermal transition of macrocyclic peptide **4** was broad: even at high temperatures, the spectra indicate that a small fraction of helix still persists, demonstrating that the thermal stability of the  $\alpha$ -helical structure was dramatically increased by self-assembly (Figure 2d).

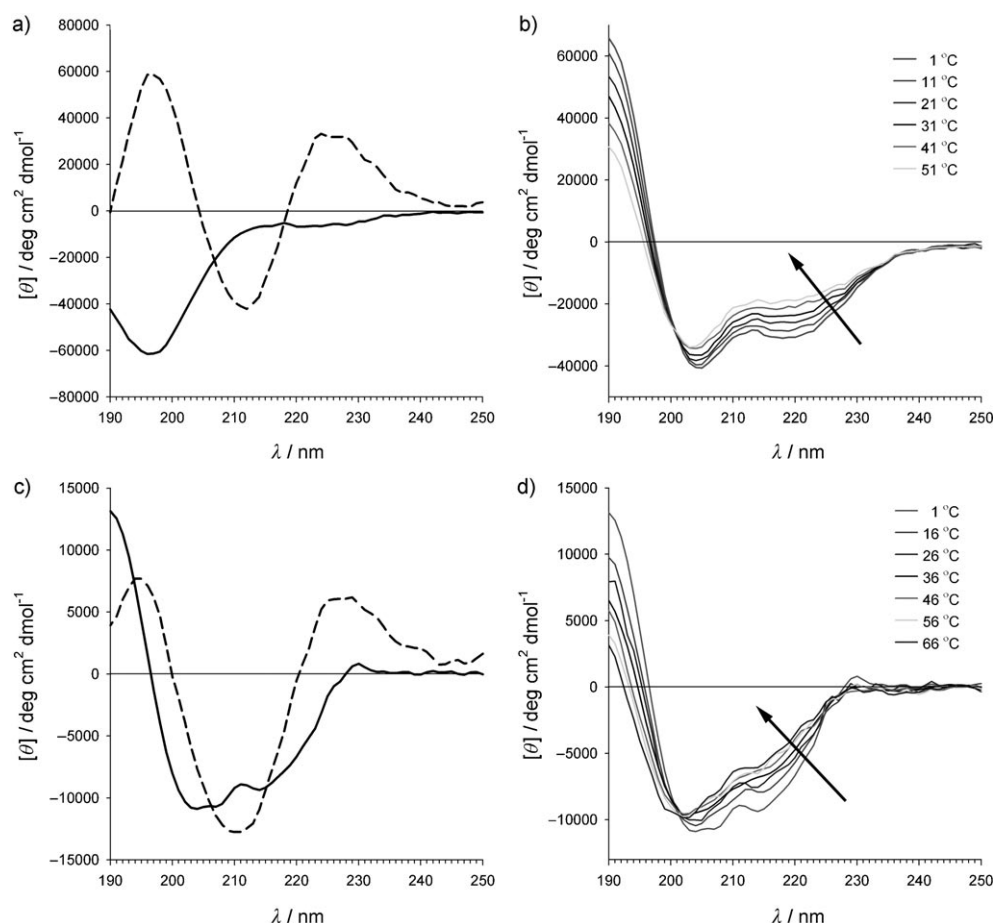


**Figure 2.** Peptide secondary-structure analyses by CD. a) Peptide **1** (—) and peptide **2** (---) in 75 mM KF at 1 °C. b) Peptide **1** in 75 mM KF, 30% TFE. c) Peptide **3** (---) and peptide **4** (—) in 75 mM KF at 1 °C. d) Effect of temperature on peptide **4** (75 mM KF).

To further scrutinize the  $\beta$ -sheet self-assembly-induced  $\alpha$ -helix stabilization process, we synthesized peptide **5** (Supporting Information, Figure S5). Peptide **5** contains the same  $\alpha$ -helix-forming segment as peptide **4**; however, mutations (Trp to Gly, and Glu to Lys) were performed on the  $\beta$ -sheet segment to prevent the peptide from forming a  $\beta$ -sheet structure. CD analysis showed that unstructured elements predominate over  $\alpha$ -helix and  $\beta$ -sheet structures (Supporting Information, Figure S7a), demonstrating the importance of  $\beta$ -sheet-induced self-assembly for helix stabilization. Cyclic peptide **7** was prepared to further exclude any possibility of coiled-coil helix bundle formation as a means to stabilize the  $\alpha$  helix. In peptide **7**, rather hydrophobic Ala residues in the helix-forming segment of peptide **4** were replaced by hydrophilic Glu residues to suppress any possibility of coiled-coil formation (Supporting Information, Figure S5). The Glu residues were positioned in such a way that Glu and Lys residues are located at  $i$  and  $i+4$  spacing. This type of arrangement places Glu and Lys residues at the same face of the  $\alpha$  helix, thus promoting salt bridge formation between oppositely charged ions. Studies have shown that peptide helices formed by this type of amino acid placement do not aggregate.<sup>[3d]</sup> As for peptide **4**, the presence of bands at 208 nm ( $\alpha$  helix), circa 215 nm ( $\beta$  sheet), and 221 nm ( $\alpha$  helix) indicates the stabilization of the  $\alpha$  helix by  $\beta$ -sheet-mediated self-assembly (Supporting Information, Figure S7b,c), thus precluding coiled-coil-mediated helix stabilization.

Transmission electron microscopy (TEM) investigations revealed that peptide **2** self-assembles into twisted fibers that are rather thick and intertwined (Figure 3a). It was difficult to exactly measure the length of the nanofibers, as they extended beyond the boundary of the high-resolution TEM image, but they were more than several micrometers long. This result is consistent with the previous reports that  $\beta$ -sheet peptides, in the absence of attached hydrophilic segments such as a polyethylene glycol (PEG) or a hydrophilic peptide, laterally associate to form hierarchical structures.<sup>[7,11]</sup> In contrast, the acyclic peptide **3** in which the hydrophilic  $\alpha$ -helix-forming segment and oligoethylene glycol-based linkers are attached to the  $\beta$ -sheet-forming segment forms discrete nanofibers that are mostly over 100 nm in length (Figure 3b).

In contrast to the formation of one-dimensional objects in the acyclic peptide **3**, the cyclic peptide **4** forms two-dimensional spherical objects along with a small number of one-dimensional objects (Figure 3c). The diameter of the spherical objects is around 10 nm. The diameter of a typical  $\alpha$  helix is circa 1.2 nm, whereas the interstrand distance between  $\beta$  strands is about 0.47 nm. Considering the fact that the  $\alpha$  helix is bulkier than the  $\beta$  strand, as noted above, helices packing side by side on a sheet would have helices rotated with respect to each other, thus promoting the formation of spherical objects (see Figure 1b). This structure is similar in appearance to the protein fold found in  $\alpha/\beta$  barrels.<sup>[12]</sup> As for the  $\alpha/\beta$  barrels, hydrophobic Trp residues on one side of the  $\beta$  tape are likely to form a hydrophobic core of the spherical objects. Taking into account of linker length (ca. 2 nm), the observed size of the spherical object is reasonable: 10 nm (the sphere diameter) = 1.2 nm  $\times$  2 (the helix diameter) + 2 nm  $\times$  2 (the linker length) + the additional contributions from

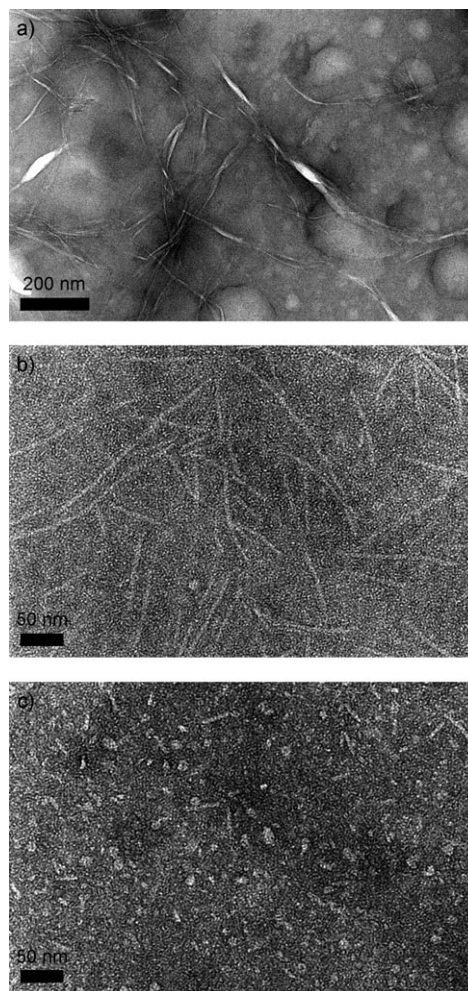


**Figure 3.** Negative-stain TEM images. a) peptide **2**, b) peptide **3**, c) peptide **4**.

$\beta$  strands and the core of the sphere. Formation of one-dimensional fibrous objects was also observed. The formation of additional one-dimensional objects can be rationalized as follows: During the self-assembly process, the formation of a double-layered  $\beta$  ribbon might precede  $\alpha$ -helix formation, which can be considered as a kinetically frozen state owing to the combination of strong interstrand  $\beta$ -sheet and intersheet hydrophobic interactions taking place over the large surface area. In such a case, the  $\alpha$ -helix-forming segment might be partially helical or unstructured within the one-dimensional objects.

Dynamic light scattering (DLS) investigations (Figure 4a) reveal that the number-weighted hydrodynamic radius distribution  $R_H$  of peptide **4** nanoaggregates is smaller than that of peptide **3** nanoaggregates, further supporting the view of the formation of smaller spherical objects than for peptide **4**. FTIR spectroscopy studies showed that both peptide **3** and peptide **4** form antiparallel  $\beta$ -sheet structures, as evidenced by the appearance of amide I bands at 1625 and 1695  $\text{cm}^{-1}$  for peptide **3**, and 1620 and 1689  $\text{cm}^{-1}$  for peptide **4** (Figure 4b,c). Contributions from  $\alpha$  helices could not be unambiguously determined owing to significant spectral overlap; however, the major difference between the spectra of peptide **3** and





**Figure 4.** a) Number-weighted hydrodynamic radius distribution  $R_H$  of peptide **3** (gray) and peptide **4** (black) by DLS. b),c) FTIR spectrum of b) peptide **3** and c) peptide **4**.

peptide **4** can be found in the amide I random-coil frequency (ca. 1640–1650  $\text{cm}^{-1}$ ).<sup>[13]</sup> The IR spectrum of peptide **3** shows that the presence of very strong random-coil bands at about 1651  $\text{cm}^{-1}$ , which dominate the contributions from other secondary structural elements. In contrast, the random-coil bands at about 1654  $\text{cm}^{-1}$  diminishes in intensity in the spectrum of peptide **4**. These results can be interpreted as the transformation of the random coil into another structure ( $\alpha$  helix) in the cyclic peptide nanoaggregates.

We next asked whether the macrocyclization approach can be applied to stabilize a biologically active  $\alpha$ -helical peptide., Rev peptide from human immunodeficiency virus type I (HIV-1) was chosen as an example of such a bioactive peptide. Rev peptide is an arginine-rich peptide that binds deeply within the major groove of the Rev response element (RRE) RNA from HIV-1 as an  $\alpha$  helix.<sup>[1b,14]</sup> It has been shown that  $\alpha$ -helix formation of Rev peptide correlates well with specific binding to RRE RNA, and the peptide is monomeric and does not aggregate.<sup>[15]</sup> Toward this end, macrocyclic peptide **11**, which contains both a minimal Rev peptide sequence (14 amino acids) and a  $\beta$ -sheet-forming segment along with other control peptides, was synthesized (Supporting Information, Figure S10). The results show that Rev peptide  $\alpha$ -helical structures can also be stabilized by  $\beta$ -sheet-mediated self-assembly of macrocyclic peptide **11**, indicating that bioactive  $\alpha$ -helix-decorated multivalent proteins can be fabricated by this approach.<sup>[16]</sup>

In conclusion, the rationally designed peptide containing  $\alpha$ -helix- and  $\beta$ -sheet-forming segments within a single macrocyclic structure self-assembles into  $\alpha$ -helix-coated nanostructures. Given that an  $\alpha$  helix at the exterior of protein is one of the key mediators of biological recognition events, our design principle can provide a good starting point for developing artificial proteins that can modulate  $\alpha$ -helix-mediated molecular recognition occurring in a multivalent fashion.<sup>[4]</sup> As the degree of  $\alpha$ -helix stabilization and biological activity should be the function of relative volume fractions of  $\alpha$ -helix,  $\beta$ -sheet, and linker segments, and other structural parameters, we are currently investigating these issues.

Received: September 23, 2008

Revised: December 12, 2008

Published online: January 22, 2009

**Keywords:** helical structures · macrocycles · nanostructures · protein models · self-assembly

- [1] a) C. O. Pabo, E. Peisach, R. A. Grant, *Annu. Rev. Biochem.* **2001**, *70*, 313–340; b) J. L. Battiste, H. Mao, N. S. Rao, R. Tan, D. R. Muhandiram, L. E. Kay, A. D. Frankel, J. R. Williamson, *Science* **1996**, *273*, 1547–1551; c) M. Uesugi, G. L. Verdine, *Proc. Natl. Acad. Sci. USA* **1999**, *96*, 14801–14806.
- [2] a) J. Liu, D. Wang, Q. Zheng, M. Lu, P. S. Arora, *J. Am. Chem. Soc.* **2008**, *130*, 4334–4337; b) M. J. Kelso, H. N. Hoang, T. G. Appleton, D. P. Fairlie, *J. Am. Chem. Soc.* **2000**, *122*, 10488–10489.
- [3] a) H. Zhang et al., *J. Mol. Biol.* **2008**, *378*, 565–580; b) F. Zhang, O. Sadowski, S. J. Xin, G. A. Woolley, *J. Am. Chem. Soc.* **2007**, *129*, 14154–14155; c) F. Ruan, Y. Chen, P. B. Hopkins, *J. Am. Chem. Soc.* **1990**, *112*, 9403–9404; d) S. Marqusee, R. L. Baldwin, *Proc. Natl. Acad. Sci. USA* **1987**, *84*, 8898–8902; e) M. Siedlecka, G. Goch, A. Ejchart, H. Sticht, A. Bierzynski, *Proc. Natl. Acad. Sci. USA* **1999**, *96*, 903–908; f) P. C. Lyu, H. X. Zhou, N. Jelveh, D. E. Wemmer, N. R. Kallenbach, *J. Am. Chem. Soc.* **1992**, *114*, 6560–6562; g) A. Verma, H. Nakade, J. M. Simard, V. M. Rotello, *J. Am. Chem. Soc.* **2004**, *126*, 10806–10807.
- [4] a) R. R. Beerli, C. F. Barbas III, *Nat. Biotechnol.* **2002**, *20*, 135–141; b) C. Jain, J. G. Belasco, *Mol. Cell* **2001**, *7*, 603–614; c) A. M. Gamper, R. G. Roeder, *Mol. Cell. Biol.* **2008**, *28*, 2517–2527.
- [5] a) Y.-b. Lim, K.-S. Moon, M. Lee, *J. Mater. Chem.* **2008**, *18*, 2909–2918; b) L. L. Kiessling, J. E. Gestwicki, L. E. Strong, *Angew. Chem.* **2006**, *118*, 2408–2429; *Angew. Chem. Int. Ed.* **2006**, *45*, 2348–2368; c) Y.-b. Lim, E. Lee, M. Lee, *Angew. Chem.* **2007**, *119*, 9169–9172; *Angew. Chem. Int. Ed.* **2007**, *46*, 9011–9014.
- [6] S. Marqusee, V. H. Robbins, R. L. Baldwin, *Proc. Natl. Acad. Sci. USA* **1989**, *86*, 5286–5290.
- [7] a) Y.-b. Lim, E. Lee, Y.-R. Yoon, M. S. Lee, M. Lee, *Angew. Chem.* **2008**, *120*, 4601–4604; *Angew. Chem. Int. Ed.* **2008**, *47*, 4525–4528; b) Y.-b. Lim, E. Lee, M. Lee, *Angew. Chem.* **2007**, *119*, 3545–3548; *Angew. Chem. Int. Ed.* **2007**, *46*, 3475–3478; c) D. M. Marini, W. Hwang, D. A. Lauffenburger, S. Zhang, R. D. Kamm, *Nano Lett.* **2002**, *2*, 295–299; d) Y.-b. Lim, S. Park, E. Lee, H. Jeong, J.-H. Ryu, M. S. Lee, M. Lee, *Biomacromolecules* **2007**, *8*, 1404–1408; e) H. Dong, S. E. Paramonov, L. Aulisa, E. L. Bakota, J. D. Hartgerink, *J. Am. Chem. Soc.* **2007**, *129*, 12468–12472.
- [8] N. K. Williams, E. Liepinsh, S. J. Watt, P. Prosser, J. M. Matthews, P. Attard, J. L. Beck, N. E. Dixon, G. Otting, *J. Mol. Biol.* **2005**, *346*, 1095–1108.

- [9] M. Cudic, J. D. Wade, L. Otvos, Jr., *Tetrahedron Lett.* **2000**, 41, 4527–4531.
- [10] S. Ganesh, S. Prakash, R. Jayakumar, *Biopolymers* **2003**, 70, 346–354.
- [11] a) A. Aggeli, I. A. Nyrkova, M. Bell, R. Harding, L. Carrick, T. C. B. McLeish, A. N. Semenov, N. Boden, *Proc. Natl. Acad. Sci. USA* **2001**, 98, 11857–11862; b) T. S. Burkoth, T. L. S. Benzinger, D. N. M. Jones, K. Hallenga, S. C. Meredith, D. G. Lynn, *J. Am. Chem. Soc.* **1998**, 120, 7655–7656.
- [12] a) J. A. Silverman, R. Balakrishnan, P. B. Harbury, *Proc. Natl. Acad. Sci. USA* **2001**, 98, 3092–3097; b) U. Uhlin, H. Eklund, *J. Mol. Biol.* **1996**, 262, 358–369.
- [13] D. Dieudonné, A. Gericke, C. R. Flach, X. Jiang, R. S. Farid, R. Mendelsohn, *J. Am. Chem. Soc.* **1998**, 120, 792–799.
- [14] V. W. Pollard, M. H. Malim, *Annu. Rev. Microbiol.* **1998**, 52, 491–532.
- [15] R. Tan, L. Chen, J. A. Buettner, D. Hudson, A. D. Frankel, *Cell* **1993**, 73, 1031–1040.
- [16] See the Supporting Information.
-